EUROPEAN JOURNAL OF
CARDIO-THORACIC
SURGERY

The papillary muscles as shock absorbers of the mitral valve complex. An experimental study

Thomas M. Joudinaud, Corrine L. Kegel, Erwan M. Flecher, Patricia A. Weber, Emmanuel Lansac, Ulrich Hvass and Carlos M.G. Duran

Eur J Cardiothorac Surg 2007;32:96-101
DOI: 10.1016/j.ejcts.2007.03.043

ELSEVIER

European Journal of Cardio-thoracic Surgery 32 (2007) 96—101

EUROPEAN JOURNAL OF CARDIO-THORACIC SURGERY

www.elsevier.com/locate/ejcts

The papillary muscles as shock absorbers of the mitral valve complex. An experimental study☆,☆☆

Thomas M. Joudinaud [a], Corrine L. Kegel [a], Erwan M. Flecher [a], Patricia A. Weber [a], Emmanuel Lansac [a], Ulrich Hvass [b], Carlos M.G. Duran [a,*]

[a] *The International Heart Institute of Montana Foundation at Saint Patrick Hospital and Health Sciences Center and The University of Montana, Missoula, Montana, USA*

[b] *Service de Chirurgie Cardiaque, Hôpital Bichat, Paris, France*

Received 3 January 2007; accepted 30 March 2007

Abstract

Objective: Although it is known that the papillary muscles ensure the continuity between the left ventricle (LV) and the mitral apparatus, their precise mechanism needs further study. We hypothesize that the papillary muscles function as shock absorbers to maintain a constant distance between their tips and the mitral annulus during the entire cardiac cycle. **Materials and methods:** Sonomicrometry crystals were implanted in five sheep in the mitral annulus at the trigones (T1 and T2), mid anterior annulus (AA) mid posterior annulus (PA), base of the posterior lateral scallops (P1 and P2), tips of papillary muscles (M1 and M2), and LV apex. LV and aortic pressures were simultaneously recorded and used to define the different phases of the cardiac cycle. **Results:** No significant distance changes were found during the cardiac cycle between each papillary muscle tip and their corresponding mitral hemi-annulus: M1—T1, ($3.5 \pm 2\%$); M1—P1 ($5 \pm 2\%$); M1—PA ($5 \pm 3\%$); M2—T2 ($2.7 \pm 2\%$); M2—P2 ($6.1 \pm 3\%$); and M2—AA ($4.2 \pm 3\%$); ($p > 0.05$, ANOVA). Significant changes were observed in distances between each papillary muscle tip and the contralateral hemi-mitral annulus: M1—T2 ($1.7 \pm 3\%$); M1—P2 ($23 \pm 6\%$); M1—AA ($6 \pm 3\%$); M2—T1 ($8 \pm 3\%$); M2—P1 ($10.5 \pm 6\%$); and M2—PA ($12.6 \pm 8\%$); ($p < 0.05$ ANOVA). The distance changes between LV apex and each papillary muscle tip were significantly different: apex—M1 ($12.9 \pm 1\%$) and apex—M2 ($10.5 \pm 1\%$) and different from the averaged distance change between the LV apex and each annulus crystal ($8.3 \pm 1\%$) with $p < 0.05$. **Conclusion:** The papillary muscles seem to be independent mechanisms designed to work as shock absorbers to maintain the basic mitral valve geometry constant during the cardiac cycle.

Keywords: Anatomy; Mitral valve; Regurgitation; Papillary muscles; Surgery

1. Introduction

Anchored to the left ventricular wall (LV) through the trabeculae carneae of the myocardium, the function of the mitral papillary muscles (PM) is to maintain the continuity between the LV wall and the mitral annulus. While it is well known that rupture of a papillary head or its elongation results in significant mitral regurgitation (MR) [1,2], the experimentally induced damage, ischemia or infarction of an isolated PM does not induce MR [3]. On the other hand, MR develops in the chronic phase of ethanol injection into the PM [4]. Papillary muscle dysfunction is only responsible for MR if a large underlying myocardium wall damage is present [5,6]. However, although papillary muscle function has been understood as the passive anchoring point of the chordae tendinae to the LV wall, recent work on ischemic MR has shown that patients with reduced PM capacity for shortening had the most severe MR [7]. Moreover, Messas et al. [8] have shown that PM contractile dysfunction can paradoxically decrease ischemic MR by PM elongation that reduces leaflet tethering and consequently improving leaflet coaptation. All these studies suggest that the PM have a far more active and complex function during the cardiac cycle than previously thought. The goal of this study was to investigate whether the PM are just a connection between chordae tendinae and left ventricular wall or an independent structure designed as a shock absorber to maintain a constant distance between their tips and the mitral annulus. This concept should have significant surgical implications.

☆ Presented at the Third Biennial Meeting of the Society of Heart Valve Disease, Vancouver, CA, June 17—20, 2005.

☆☆ Thomas Joudinaud was supported by Club des Coeurs Ouverts (CCO), Paris, France, and a grant from The International Heart Institute of Montana Foundation. Erwan Flecher was supported by Association Chirurgicale pour le Développement et l'amélioration des Techniques de dépistage et de traitement des maladies Cardio-vasculaires (ADETEC) and a grant from Assistance Publique-Hôpitaux de Paris.

* Corresponding author. The International Heart Institute of Montana Foundation, 554 West Broadway, Missoula, MT 59802, USA. Tel.: +1 406 329 5668; fax: +1 406 329 5880.

E-mail address: duran@saintpatrick.org (C.M.G. Duran).

1010-7940/$ — see front matter
doi:10.1016/j.ejcts.2007.03.043

2. Materials and methods

All animals were cared for in accordance with the 'Principles of Laboratory Animal Care' formulated by the National Society of Medical Research and the 'Guide for the Care and Use of Laboratory Animals' prepared by the Institute of Animal Resources, National Research Council, and published by the National Academy Press, revised 1996. The protocol for the use of the animals for this project was also reviewed and approved by the Institutional Animal Care and Use Committee (IACUC) of The University of Montana.

2.1. Surgical protocol

Targhee sheep underwent implantation of nine ultrasonic crystals on the mitral valve apparatus using cardiopulmonary bypass. The animal was placed in the right lateral decubitus position on the operating table and a left jugular catheter was placed. The animal was premedicated with intravenous (I.V.) administration of ketamine 1.0 mg/kg, atropine 0.03 mg/kg, and propofol 4.0 mg/kg. Artificial ventilation was maintained with a volume respirator (North American Drager, Telford, PA, USA) supplemented with oxygen at 4 l/min. Anesthesia was maintained with intermittent propofol and continuous isoflurane (1.5—2.5%). A Swan-Ganz catheter was introduced through the left jugular vein into the pulmonary artery. At baseline, three consecutive sets of measurements of cardiac output and right ventricular (RV) and pulmonary artery pressures were taken. EKG was monitored throughout the experiment.

The heart was exposed with a T-shaped incision of the pericardium through a standard left thoracotomy into the 4th intercostal space. The heart was then suspended in a pericardial cradle. Heparin 300 U/kg I.V. was injected as a bolus in preparation for cardiopulmonary bypass with a target ACT of 480 s or above. The ascending aorta was cannulated with a #16-Fr Medtronic arterial cannula. A #32-Fr cannula was inserted into the inferior vena cava and a #24-Fr into the superior vena cava.

Cardiopulmonary by-pass (CPB) was then instituted. Two cotton umbilical tapes were placed around the superior and inferior vena cavae. A LV vent line was inserted into the LV apex. The ascending aorta was cross-clamped followed by infusion of cold crystalloid cardioplegia into the aortic root.

2.2. Surgical implantation of crystals

Nine ultrasonic crystals (Sonometrics, London, Ontario, Canada) were implanted in each sheep. One crystal was implanted at the apex of the LV and another close to the tip of each PM at the easily identified point of insertion of the anterior strut basal chords (M1, M2). The electrodes of these two crystals were exteriorized through the ventricular wall. Six other crystals were secured on the mitral valve annulus at the right (T1) and left (T2) trigones; mid-point of the anterior annulus (AA); mid-point of the posterior annulus (PA); and at the bases of each posterior lateral scallops (P1 and P2); (Fig. 1). These electrodes were exteriorized through the left atriotomy. Two high fidelity catheter-tipped pressure transducers (model 510, Millar Instruments, Houston, TX) were placed within the lumen of the proximal ascending aorta (Ao) and the LV cavity through the apex.

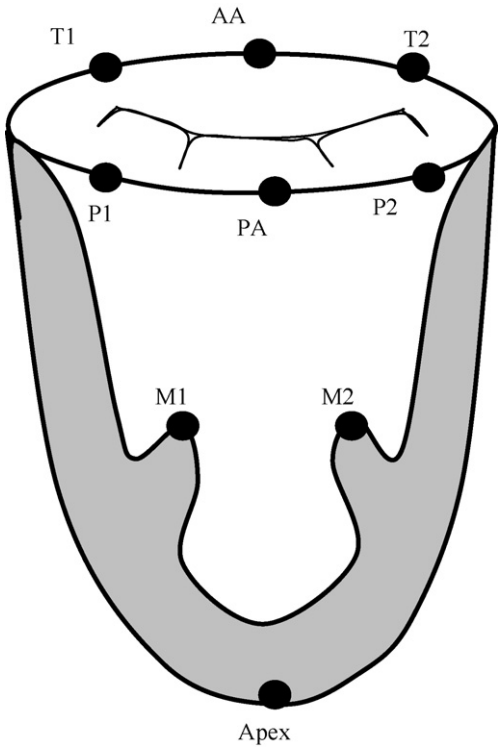

Fig. 1. Locations of the sonomicrometry crystals on the mitral annulus and papillary muscles. AA: mid-anterior annulus; PA: mid-posterior annulus; T1: left trigone; T2: right trigone; P1: base of antero-lateral scallop of posterior leaflet; P2: base of postero-lateral scallop of posterior leaflet; M1: tip of antero-lateral papillary muscle; M2: tip of postero-medial papillary muscle.

2.3. Data acquisition

After discontinuing CPB, and after the animal was hemodynamically stable (minimum >15 min), crystal distances, LV, and aortic pressures were simultaneously recorded. Epicardial two-dimensional (2-D) echocardiography with color Doppler was used to assess the competence and anatomy of the mitral valve. At the end of the experiment, the heart was arrested by lethal injection of potassium chloride and explanted from the body cavity. The correct position of the crystals was checked.

2.4. Data analysis

A post-processing program (Sonometrics Corporation, London, Ontario, Canada) was used to examine each individual length tracing between crystals. Data sampling rate was 200 Hz. A filter algorithm eliminated possible signal corruption by analyzing the pattern of both the true distance and the corrupted data. Millar pressure transducer control units TCB 600 and MIKRO-TIP pressure transducers (Millar Instruments Inc. Houston, TX, USA) were used to obtain the LV and Ao pressures. All distances and pressures were displayed and recorded simultaneously on the same screen by the sonometrics system. This ensures that all data are synchronized and recorded at the same timeline.

Table 1
Variations in distances between M1–mitral annulus and M2–mitral annulus during the cardiac cycle

	IVC	Ej	IVR	D	MidD
M1–P1	26.21 ± 1.39	26.86 ± 1.81	26.94 ± 1.79	27.22 ± 2.16	26.35 ± 1.58
M1–T1	28.60 ± 3.09	28.45 ± 2.71	28.58 ± 2.44	28.62 ± 3.16	28.68 ± 3.21
M1–AA*	32.90 ± 1.40**	33.01 ± 1.21‡	32.06 ± 0.88	31.64 ± 1.59	32.68 ± 1.45
M1–T2*	36.94 ± 2.46**,***	36.51 ± 1.94†,‡	33.58 ± 1.12#	34.06 ± 2.69	35.88 ± 3.26
M1–P2*	37.68 ± 4.05**	36.96 ± 4.21	32.10 ± 7.05	34.71 ± 5.71	37.86 ± 5.31
M1–PA	33.14 ± 2.01	34.27 ± 1.68	33.39 ± 0.63	32.85 ± 1.63	33.18 ± 1.84
M2–PA*	31.89 ± 2.79**	34.61 ± 3.33	35.04 ± 3.05	33.40 ± 3.55	31.80 ± 4.03
M2–P1*	39.75 ± 2.06**	39.34 ± 1.89	36.24 ± 0.52	38.81 ± 1.08	38.84 ± 2.85
M2–T1*	43.08 ± 0.87**	41.06 ± 1.55	39.98 ± 2.42	40.49 ± 1.62	41.20 ± 0.92
M2–AA	38.04 ± 2.00	37.78 ± 2.67	38.25 ± 2.35	37.98 ± 2.35	37.50 ± 1.52
M2–T2	29.72 ± 2.65	30.08 ± 2.63	30.20 ± 2.35	29.81 ± 2.50	29.68 ± 2.58
M2–P2	26.37 ± 2.77	27.29 ± 2.79	28.03 ± 2.52	26.81 ± 2.60	26.51 ± 2.92

IVC: isovolumic contraction; Ej: ejection; IVR: isovolumic relaxation; D: end IVR; midD: mid point between D and IVC. Significant Bonferroni/Dunn test with $p < 0.05$.
* $p < 0.05$ (repeated-measures ANOVA).
** IVC versus IVR.
*** IVC versus D.
† Ejection versus isovolumic relaxation.
‡ Ejection versus D.
# Isovolumic relaxation versus mid diastole.

2.5. Definition of the different phases of the cardiac cycle

The different phases of the cardiac cycle were defined from the LV and Ao pressure curves. End diastole or beginning of systole (isovolumic contraction or IVC) was defined as the beginning of increasing of LVP ($dP/dt > 0$). End of IVC was defined as the beginning of ejection (Ej) on the crossing point of LV and Ao pressures (gradient AoP/LVP = 0). The dichrotic notch on the Ao pressure curve defined end-ejection time and beginning of isovolumic relaxation (IVR). End of IVR was defined by the lowest pressure point of the LV pressure curve (D). The mid-time point between D and the beginning of systole defined mid-diastole point (midD).

2.6. Measurements and statistical analysis methods

After examination of the data, three consecutive heartbeats that contained the least amount of noise were chosen for analysis for each animal. Once these calculations were complete, summaries were reported for each location as mean ± 1SD (one standard deviation).

The distance changes between each papillary muscle tip and each crystal of the mitral annulus (M1–mitral annulus and M2–mitral annulus), between LV apex and each papillary muscle tip (apex–M1 and apex–M2) and between the apex and the crystals on the mitral annulus (apex–mitral annulus) were recorded during the cardiac cycle. The distance changes throughout the cardiac cycle were analyzed by repeated measures ANOVA with $p < 0.05$ considered as significant. Bonferroni test was used to analyze the significant variations between the different time of analysis with $p < 0.01$ significance level. The distances between the apex and each annulus crystals were averaged and comparison between the changes in apex–mitral annulus average distance and apex–M1 and apex–M2 was made with the unpaired student t-test. $p < 0.05$ was considered significant.

3. Results

Five Targhee sheep (78 ± 12 kg) underwent the placement of nine crystals on the mitral valve. The hemodynamic characteristics at the time of recording were as follows: arterial pressure 67/40 ± 2/3 mmHg, cardiac output 2.9 ± 0.4 l/min, pulmonary artery pressure 20/11 ± 1/1 mmHg. No mitral or tricuspid regurgitation were detected in epicardial echocardiography at the time of recording. At necropsy, all crystals in the mitral annulus and papillary muscles were in the correct position. Average pump time

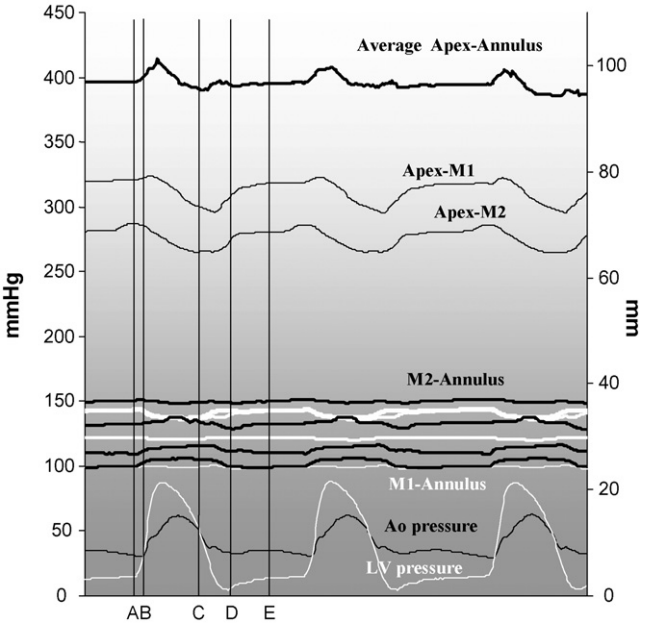

Fig. 2. Variations through the cardiac cycle of the distances: Average apex–mitral annulus, apex–M1 and M2 and M1 and M2–mitral annulus (Sheep number 3). Flat lines showing no significant distance variation during the cardiac cycle of M1 and M2 to their corresponding hemi-annulus (A = IVC; B = EJ; C = IVR; D = mid D; E = D).

was 136 ± 9 min and average cross-clamp time was 88 ± 6 min.

The changes in distances between the anterior (M1) and posterior (M2) papillary muscles and the mitral annulus are shown in Table 1. During the cardiac cycle there were no significant changes in distance between the anterior papillary muscle tip and the anterior mitral hemi-annulus: M1–T1 (3.5 ± 2%, $p = 0.9751$), M1–P1 (5 ± 2%, $p = 0.0681$), and M1–PA (5 ± 3%, $p = 0.4148$). Significant changes were observed in distances between the anterior papillary tip and the posterior mitral hemi-annulus: M1–T2 (11.7 ± 3%; $p = 0.0006$), M1–P2 (23 ± 6%; $p = 0.0069$), and M1–AA (6 ± 3%; $p = 0.0094$). These significant changes occurred mostly between IVC and D phases of the cardiac cycle for M1–T2 and M1–P2 (−10 ± 4%, $p = 0.0008$ and −20 ± 5%, $p = 0.002$, respectively) and between IVR and midD (6.4 ± 4%, $p = 0.0007$ and 15.5 ± 8%, $p = 0.004$, respectively).

The changes in distance between M2–T2 (2.7 ± 2% $p = 0.24$), M2–P2 (6.1 ± 3%, $p = 0.07$), and M2–AA (4.2 ± 3%, $p = 0.63$) were not significant. However, significant changes in distance between M2–T1 (8 ± 3%, $p = 0.04$), M2–P1 (10.5 ± 6%, $p = 0.031$), and M2–PA (12.6 ± 8%, $p = 0.0039$) were observed. These significant changes occurred mostly between beginning of IVC and end of ejection for M2–T1, M2–P1 and M2–PA (−6 ± 5%, $p = 0.003$; −10 ± 6%, $p = 0.004$; and +9 ± 5%, $p = 0.002$, respectively).

Fig. 2 shows the variations in distance between the LV apex and both papillary muscle tips (apex–M1 and apex–M2) and to the mitral annulus (average apex–annulus) during the cardiac cycle. The flat tracings of the changes in distances between papillary muscles tips and mitral annulus during the cardiac cycle show that there are almost no variations in distance. In comparison, variations in distance between LV apex–papillary muscle tips and apex–mitral annulus are greater.

There were significant changes in distances between apex–M1, apex–M2 (12.9 ± 1%, $p = 0.021$ and 10.5 ± 1%, $p = 0.0016$, repeated measures ANOVA, respectively), and between apex and the annulus crystals (8.3 ± 1%, $p < 0.001$, repeated measures ANOVA). Distance variations during the five time points of the cardiac cycle are presented in Table 2. During the cardiac cycle, the apex–annulus maximum changes were significantly different from the changes between apex–M1 ($p = 0.002$) and apex–M2 ($p = 0.017$). During IVC, apex–annulus, apex–M1, and apex–M2 increased (Table 2 and Fig. 2), although the percentage of expansion were significantly different ($p = 0.01$, for apex–annulus vs apex–M1 and apex–M2). During the ejection period, apex–annulus reached its maximum value and started to decrease until the IVR phase during which it reached its minimum value. Apex–M1 and apex–M2 tracings followed the similar trend of apex–annulus tracings. During the other phases of the cardiac cycle, no significant differences were found in the distance changes between apex–annulus and apex–M1 or apex–M2. However, we observed in the time tracings that during IVR, apex–annulus increased and then decreased until D, while apex–M1 and apex–M2 were increasing.

Table 2
Changes in average distances between apex–annulus, apex–M1, and apex–M2 during the cardiac cycle

		Average change (%)		Bonferoni/ Dunn test (p)
Apex–annulus				
IVC	88.50 ± 4.33	IVC versus Ej	5.2 ± 1	0.0001
Ej	92.46 ± 4.02	Ej versus IVR	−8.3 ± 2	0.0001
IVR	86.19 ± 5.66	IVR versus D	1.5 ± 1	0.035
D	85.21 ± 5.95	D versus midD	−0.9 ± 0.6	0.096
MidD	87.12 ± 5.28	MidD versus IVC	2.1 ± 1	0.93
Apex–M1				
IVC	46.13 ± 3.21	IVC versus Ej	1 ± 4	0.81
Ej	47.06 ± 3.52	Ej versus IVR	−7 ± 5	0.0011
IVR	43.20 ± 2	IVR versus D	1 ± 3	0.6
D	41.32 ± 3.7	D versus midD	4 ± 3	0.035
MidD	44.13 ± 4.01	MidD versus IVC	2 ± 1	0.12
Apex–M2				
IVC	33.82 ± 3.85	IVC versus Ej	0.8 ± 2	0.001
Ej	35.28 ± 3.48	Ej versus IVR	−8 ± 2	0.002
IVR	32.79 ± 3.29	IVR versus D	1 ± 3	0.007
D	31.01 ± 4.03	D versus midD	7 ± 6	0.0012
MidD	33.84 ± 2.5	MidD versus IVC	2 ± 0.5	0.91

4. Discussion

Morphologically, the papillary muscles can be considered as myocardial protuberances of the LV wall. Their muscular fibers of the body and base suggest a direct continuity with the myocardium of the LV. However, using X-ray multi-detector CT with interactive 3-D images, Axel [9] has shown that the base of the human papillary muscles is not in continuity with the LV wall but through trabeculae carneae with clear demarcation spaces between both structures. These facts suggest that anatomically, the papillary muscles are different from the LV wall.

Sakai and associates [10] have shown in a human necropsy study that the distances between the papillary muscle tips and the corresponding trigones and between the papillary muscle tips and the corresponding posterior annulus at the level of the bases of the lateral scallops were equal. It has also been shown in dogs under different heart rates and preload conditions, that the orthogonal distance between the plane of the mitral annulus and the tips of both papillary muscles had a variation smaller than 1-mm during the cardiac cycle [11]. In the same study, using the center of the mitral annulus as the origin of a coordinate system, these authors showed an elongation followed by shortening of the papillary muscle length during systole. Our results confirm these findings. In the present study, we also observed that the distance between the tip of each papillary muscle and the corresponding hemi-mitral annulus remained constant during the whole cardiac cycle. An interesting finding is that the distance between the anterior papillary muscle (M1) and anterior annulus (AA) and the distance between the posterior papillary muscle (M2) and posterior annulus (PA) presented significant changes. Simultaneously, the distance between anterior papillary muscle tip (M1) and mid posterior annulus (PA) and the distance between posterior papillary muscle tip (M2) and mid-point of the anterior annulus (AA) remained the same during the cardiac cycle. The constant distance between M2 and AA as well as M1 and PA may reflect the torsion of the ventricular wall during contraction.

Since it is not possible to determine the morphological apical extremity of the papillary muscles, we assumed that

the distance changes between LV apex and papillary tip corresponded (at least partially) to the changes in the elongation and shortening of the papillary muscles during the cardiac cycle. These changes were significantly different (Table 2). Furthermore, we observed that the average change in distance between apex and the mitral annulus crystals was significantly different from the distance changes between apex and papillary muscle tips. This was more apparent during IVC. We also observed that the changes in the tracings of apex to both papillary muscle tips (apex–M1 and apex–M2) were different from apex–annulus during IVR. These significant differences between apex–annulus and apex–tips of papillary muscle distance changes show that both papillary muscle tips do not follow the LV wall contraction. The papillary muscles cannot be simply understood as passive anchorage points between the mitral chords and the LV wall but rather function as an active shock absorber independent from the LV wall designed to maintain a constant distance between each hemi-valve annulus and their corresponding chordal insertions into the tips of the papillary muscles. Since the marginal chords shape and tension change continuously during the cardiac cycle, they cannot be the mechanism responsible for maintaining constant this annulo-papillary distance. Only the basal chords and in particular the two, thick anterior and posterior strut or stay chords can support this annulo-papillary distance. These two stay chords remain taught during the whole cardiac cycle [12] and Lomholt et al. [13] have shown that they sustain three times more tension than the corresponding marginal chords. Rodriguez et al. [14] and Goetz et al. [15] have shown experimentally that these stay chords are not only essential for maintaining LV geometry but more importantly, for its function.

4.1. Clinical implications

The present study confirms previous reports that showed that the distance between tips of papillary muscles and the mitral annulus remain constant during the normal cardiac cycle [11]. While the annulo-papillary distance does not change, the distance between the annulus and LV apex changes continuously. The underlying mechanism responsible for these findings was unknown. The present study suggests that while the practically inextensible basal chords connect the papillary muscles to the mitral annulus, the papillary muscles function as shock absorbers compensating for the pull of the changing LV wall. They are anatomically and functionally distinct from the LV wall. The above findings might explain the well known deleterious effect of loosing the annulo-papillary continuity observed after total mitral replacement [16]. Although the standard solution has been to conserve as much as possible of the whole mitral valve, it is difficult to understand how the marginal chords can play such an important role. Our present findings suggest that it is only the basal chords that should be conserved. If this is not possible because of the total distortion of the mitral apparatus, new stay chords should be used.

Recently, Levine [17] has shown that the main cause of ischemic mitral regurgitation is the tethering of the leaflets by the apico-lateral pull of the stay chords. The same group has logically suggested the section of the two anterior stay chords to free the tethered leaflet's body and shown that it abolishes the regurgitation [18]. This technique has been applied to a few clinical cases but its results are not yet available. However, several authors have shown experimentally that section of the two anterior basal stay chords while not inducing mitral regurgitation, results in an increase in the distance between apex to trigones and tips of papillary muscles to trigones [14]. The mitro-aortic angle also became more acute as if unsupported by the stay chords [19]. These geometric changes were associated with local systolic strain distortion affecting micro-torsion, wall-thickening, and global systolic dysfunction [20]. It is therefore unlikely that cutting the anterior stay chords can be done with impunity. In our opinion, it is far more physiologic to place new artificial stay chords. By approximating the papillary muscles to the trigones, the body of the anterior leaflet is free to regain its normal shape.

4.2. Study limitations

Although sonomicrometry has an outstanding spatial and temporal resolution [21], variability in the surgical placement of the crystals and anatomic variations of the animals can explain the important standard deviations observed. In order to minimize this problem, the same surgeon performed all surgeries. The small number of animals is obviously a major limitation of this study. This experiment was conducted as an acute, open chest, open pericardium study on an anesthetized animal. These limitations associated with the deleterious effect of cardio-pulmonary bypass and ischemia might have resulted in abnormal myocardial and valve behavior. Also, the absence of a crystal at the base of the papillary muscles made impossible to measure their actual changes. However, determination of the exact location of the papillary base is close to impossible while that of their tips is easy. In spite of these limitations, the basic similarities of our data with those previously reported by other authors give strength to our findings. Whether these findings in sheep can be applied to the human remains unknown.

5. Conclusion

The papillary muscles are anatomically and functionally distinct from the LV wall. They function as a shock absorber that compensates for the geometric changes of the LV wall while maintaining their tips at a constant distance to their corresponding mitral hemi-annulus. While this distance does not vary during the cardiac cycle, the apex to mitral annulus distances changes significantly at the expense of the changes in the apex to papillary muscle tips. The reason for this annulo-papillary stability is probably due to the presence of the anterior basal stay chords. These findings should enhance new surgical techniques for the conservation of annulo-papillary continuity and the repair of functional mitral regurgitation.

Acknowledgements

We appreciate the editorial assistance of Jill Roberts.

References

[1] Burch GE, De Pasquale NP, Phillips JH. Clinical manifestations of papillary muscle dysfunction. Arch Intern Med 1963;112:112—7.

[2] Voci P, Bilotta F, Caretta Q, Mercanti C, Marino B. Papillary muscle perfusion pattern. A hypothesis for ischemic papillary muscle dysfunction. Circulation 1995;91(6):1714—8.

[3] Kaul S, Spotnitz WD, Glasheen WP, Touchstone DA. Mechanism of ischemic mitral regurgitation. An experimental evaluation. Circulation 1991;84(5):2167—80.

[4] Tsakiris AG, Rastelli GC, Amorim Dde S, Titus JL, Wood EH. Effect of experimental papillary muscle damage on mitral valve closure in intact anesthetized dogs. Mayo Clin Proc 1970;45(4):275—85.

[5] Fischer GC, Wessel HU, Sommers HM. Mitral insufficiency following experimental papillary muscle infarction. Am Heart J 1972;83(3):382—9.

[6] Llaneras MR, Nance ML, Streicher JT, Lima JA, Savino JS, Bogen DK, Deac RF, Ratcliffe MB, Edmunds Jr LH. Large animal model of ischemic mitral regurgitation. Ann Thorac Surg 1994;57(2):432—9.

[7] Kisanuki A, Otsuji Y, Kuroiwa R, Murayama T, Matsushita R, Shibata K, Yutsudo T, Nakao S, Nomoto K, Tomari T. Two-dimensional echocardiographic assessment of papillary muscle contractility in patients with prior myocardial infarction. J Am Coll Cardiol 1993;21(4):932—8.

[8] Messas E, Guerrero JL, Handschumacher MD, Chow CM, Sullivan S, Schwammenthal E, Levine RA. Paradoxic decrease in ischemic mitral regurgitation with papillary muscle dysfunction: insights from three-dimensional and contrast echocardiography with strain rate measurement. Circulation 2001;104(16):1952—7.

[9] Axel L. Papillary muscles do not attach directly to the solid heart wall. Circulation 2004;109(25):3145—8.

[10] Sakai T, Okita Y, Ueda Y, Tahata T, Ogino H, Matsuyama K, Miki S. Distance between mitral anulus and papillary muscles: anatomic study in normal human hearts. J Thorac Cardiovasc Surg 1999;118(4):636—41.

[11] Komeda M, Glasson JR, Bolger AF, Daughters 2nd GT, Ingels Jr NB, Miller DC. Papillary muscle-left ventricular wall ''complex''. J Thorac Cardiovasc Surg 1997;113(2):292—300. discussion 300—1.

[12] van Rijk-Zwikker GL, Delemarre BJ, Huysmans HA. Mitral valve anatomy and morphology: relevance to mitral valve replacement and valve reconstruction. J Card Surg 1994;9(2 Suppl.):255—61.

[13] Lomholt M, Nielsen SL, Hansen SB, Andersen NT, Hasenkam JM. Differential tension between secondary and primary mitral chordae in an acute in-vivo porcine model. J Heart Valve Dis 2002;11(3):337—45.

[14] Rodriguez F, Langer F, Harrington KB, Tibayan FA, Zasio MK, Cheng A, Liang D, Daughters GT, Covell JW, Criscione JC, Ingels NB, Miller DC. Importance of mitral valve second-order chordae for left ventricular geometry, wall thickening mechanics, and global systolic function. Circulation 2004;110(11 Suppl. 1):II115—22.

[15] Goetz WA, Lim HS, Lansac E, Saber HA, Pekar F, Weber PA, Duran CM. Anterior mitral basal 'stay' chords are essential for left ventricular geometry and function. J Heart Valve Dis 2005;14(2):195—202. discussion 202—3.

[16] David TE. Mitral valve replacement with preservation of chordae tendinae: rationale and technical considerations. Ann Thorac Surg 1986;41(6):680—2.

[17] Levine RA. Dynamic mitral regurgitation—more than meets the eye. N Engl J Med 2004;351(16):1681—4.

[18] Messas E, Guerrero JL, Handschumacher MD, Conrad C, Chow CM, Sullivan S, Yoganathan AP, Levine RA. Chordal cutting: a new therapeutic approach for ischemic mitral regurgitation. Circulation 2001;104(16):1958—63.

[19] Goetz WA, Lim HS, Lansac E, Weber PA, Birnbaum DE, Duran CM. The aortomitral angle is suspended by the anterior mitral basal ''stay'' chords. Thorac Cardiovasc Surg 2003;51(4):190—5.

[20] Rodriguez F, Langer F, Harrington KB, Tibayan FA, Zasio MK, Liang D, Daughters GT, Ingels NB, Miller DC. Cutting second-order chords does not prevent acute ischemic mitral regurgitation. Circulation 2004;110(11 Suppl. 1):II91—7.

[21] Gorman 3rd JH, Gupta KB, Streicher JT, Gorman RC, Jackson BM, Ratcliffe MB, Bogen DK, Edmunds Jr LH. Dynamic three-dimensional imaging of the mitral valve and left ventricle by rapid sonomicrometry array localization. J Thorac Cardiovasc Surg 1996;112(3):712—26.

The papillary muscles as shock absorbers of the mitral valve complex. An experimental study

Thomas M. Joudinaud, Corrine L. Kegel, Erwan M. Flecher, Patricia A. Weber, Emmanuel Lansac, Ulrich Hvass and Carlos M.G. Duran

Eur J Cardiothorac Surg 2007;32:96-101
DOI: 10.1016/j.ejcts.2007.03.043